PERMSELECTIVITY OF THE GLOMERULAR CAPILLARY WALL TO MACROMOLECULES

I. THEORETICAL CONSIDERATIONS

RAMSAY L. S. CHANG, CHANNING R. ROBERTSON, WILLIAM M. DEEN, *and* BARRY M. BRENNER

From the Kidney Research Laboratory, Veterans Administration Hospital, San Francisco, California 94121; the Department of Chemical Engineering, Stanford University, Stanford, California 94305; and the Departments of Medicine and Physiology and the Cardiovascular Research Institute of the University of California, San Francisco, California 94143

ABSTRACT The transport of macromolecules across the renal glomerular capillary wall has been described theoretically using flux equations based on (*a*) restricted transport through small pores, and (*b*) the Kedem-Katchalsky formulation. The various assumptions and limitations inherent in these two approaches are discussed. To examine the coupling between macromolecular solute transport and the determinants of glomerular filtration rate, these flux equations were combined with mass balance relations which allow for variations in the transmembrane driving forces along a glomerular capillary. It was predicted, using both pore theory and the Kedem-Katchalsky equations, that fractional solute clearance should be strongly dependent on the determinants of glomerular filtration rate when convection and diffusion both contribute to solute transport. When convection becomes the sole mechanism for transcapillary solute transport, however, fractional solute clearance is essentially independent of changes in the determinants of glomerular filtration rate. Consequently, unless diffusion is absent, fractional solute clearances alone are insufficient to characterize the permselective properties of the glomerular capillary wall, since these values may be altered by changes in glomerular pressures and flows as well as changes in the properties of the capillary wall per se.

INTRODUCTION

One of the most remarkable features of the glomerular filtration process is the extent to which the glomerular capillary wall discriminates among molecules of varying size. Uncharged molecules the size of inulin or smaller normally appear in glomerular ultrafiltrate in the same concentrations as in plasma water, whereas the transport of substances of increasingly greater size diminishes progressively, normally reaching very low values as the size of serum albumin is approached. For this reason, all but the smallest plasma proteins are normally restricted from passage into Bowman's space, the proximal-most portion of the renal tubule. In addition to size, it seems likely that

molecular charge as well as other physical and chemical properties of macromolecules will also influence this permselectivity.

In an effort to understand the mechanisms governing the transport of macromolecules, it is important to recognize that solute and water transport across the glomerular capillary are coupled. In particular, Pappenheimer, Renkin, Lambert, and their respective co-workers (1–4) have derived equations which show that the Bowman's space to plasma concentration ratio of a macromolecule depends inversely on glomerular filtration rate (GFR). Accordingly, the transport of macromolecules will be influenced not only by the physicochemical properties of the capillary wall, but also by the other determinants of GFR, namely, the transcapillary hydraulic and oncotic pressure differences and the glomerular capillary plasma flow rate. The goal of this theoretical study is to examine in greater detail how the membrane properties and the transcapillary driving forces interact to determine the transport of macromolecules.

The present approach differs from that taken previously (1–4) in two important respects. First, the effects on solute transport of variations in each of the individual determinants of GFR are considered. This is appropriate given the recent discovery of a unique strain of Wistar rats with glomeruli on the surface of the renal cortex, which makes possible direct measurement of these quantities, and hence, assessment of their individual effects on glomerular transcapillary exchange of a variety of macromolecular species. One such assessment, employing dextrans of varying molecular radius, is contained in the companion study (5). Second, variations in the driving forces for water and solute transport that must occur along a glomerular capillary are incorporated in this formulation. Our previous theoretical (6, 7) and experimental (8–16) studies of the determinants of GFR have shown, for example, that the dependence of GFR on glomerular plasma flow rate is brought about by flow-induced variations in the colloid osmotic pressure profile along a glomerular capillary. Consequently, it seems likely that variations in the solute concentration profile along a glomerular capillary, coupled to changes in glomerular plasma flow and the other determinants of GFR, will affect macromolecular solute transport. To examine these effects, mass balance equations for water and solute for the glomerular capillary network have been combined with expressions for water and solute fluxes based on either the Kedem-Katchalsky formulation or the hydrodynamic theory of solute transport through pores. Both sets of flux equations are commonly used in characterizing membrane transport processes and are consistent with the postulates of nonequilibrium thermodynamics, but they differ sufficiently to merit a comparison of the two approaches.

MODEL DEVELOPMENT

Thermodynamic Basis of Flux Equations

Essential to a thermodynamic description of mass transport through membranes is an expression for the local rate of entropy production at any point within the membrane. For a one-dimensional, isothermal system in the absence of chemical reaction, assuming local equilibrium (a postulate of nonequilibrium thermodynamics), this can be

written as follows (17):

$$\phi = -\sum_{i=1}^{n} N_i(d\mu_i/dz), \tag{1}$$

where ϕ, the dissipation function per unit volume, is the product of the volumetric rate of entropy production and the absolute temperature, N_i is the molar flux of species i relative to the mass average velocity, μ_i is the chemical potential of species i, and z is a coordinate perpendicular to the plane of the membrane. In further accord with the postulates of nonequilibrium thermodynamics, the fluxes (N_i) are related to the driving forces ($d\mu_i/dz$) in a linear manner (17):

$$N_i = \sum_{j=1}^{n} \alpha_{ij}(d\mu_j/dz) \qquad i = 1, 2, \ldots n, \tag{2}$$

where α_{ij} are phenomenological coefficients with the property that $\alpha_{ij} = \alpha_{ji}$ (Onsager reciprocity relation). Eqs. 1 and 2 form the common basis for both sets of flux equations employed in the analysis that follows.

In the development of the flux equations it will be sufficient to consider a ternary system composed of water, an uncharged macromolecular solute, and the membrane. Since it has been shown experimentally (18) that the glomerular capillary wall is essentially impermeable to the major plasma proteins, these will enter into the analysis only in that they contribute a transmembrane osmotic pressure difference. To relate the molar flux of species i at steady state to the transmembrane difference in μ_i, Eqs. 1 and 2 are integrated across the membrane. The flux equations based on the hydrodynamic theory of transport through pores assume the membrane to consist of an impermeable matrix perforated by a number of solvent-filled, cylindrical pores; the Kedem-Katchalsky equations are obtained by performing the necessary integration without specifying the internal structure of the membrane.

Flux Equations Derived from Pore Theory

The pioneering efforts of Pappenheimer et al. (1, 19) and Renkin (2) in the use of the theory of transport through porous membranes, and subsequent refinements of their treatments, have been discussed by Solomon (20), Bean (21), Verniory et al. (4), and Anderson and Quinn (22). This approach, in its simplest form, involves the assumption that transport takes place through a number of identical cylindrical pores of radius r_o and length l, as shown in Fig. 1. Hydrodynamic relations are utilized to specify the various frictional interactions among the solute (treated as a solid spherical particle), the solvent (treated as a continuum), and the pore wall. The expressions for volume flux (J_v) and solute mass flux (J_s) which result are:

$$J_v = (r_o^2/8\eta l)(S'/S)(\Delta P - \Delta\pi) = (k'S'/S)(\Delta P - \Delta\pi), \tag{3}$$

$$J_s = \chi_o C_o J_v[1 - (C_l/C_o)\exp(-\gamma)]/[1 - \exp(-\gamma)]. \tag{4}$$

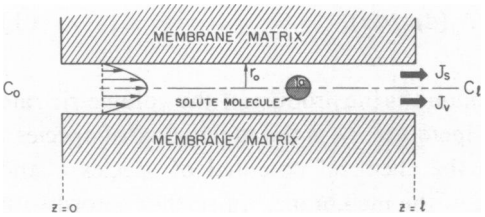

FIGURE 1

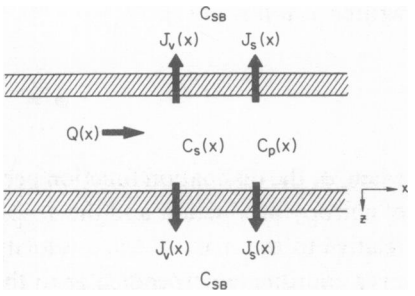

FIGURE 2

FIGURE 1 Schematic of a membrane perforated by a solvent-filled right-cylindrical pore in which the solvent velocity profile is parabolic and the solute molecule traverses the pore along the pore centerline. Symbols in this and subsequent figures are as defined in the text and List of Symbols.
FIGURE 2 Idealization of the glomerular capillary network.

For definitions of the various symbols see List of Symbols.

An important feature of Eq. 3, where it is assumed that the osmotic pressure of the permeant solute is negligible, is that the hydraulic permeability (k') is given explicitly in terms of the pore geometry (r_o, l) and solvent viscosity (η). The factor S'/S appears in Eq. 3 because J_v and J_s are based on total membrane surface area (S) rather than total pore area (S'). The quantity γ in Eq. 4 is a measure of the relative importance of convection and diffusion to solute transport within a pore (see Eq. 52). Although Eq. 4 does not contain readily identifiable terms representing the separate contributions of convection and diffusion, these can be obtained as shown in the Appendix (Eq. 51). The Appendix contains a derivation of Eqs. 3 and 4, based on Eqs. 1 and 2, together with a discussion of some fundamental assumptions inherent in this approach that have not been considered in previous treatments (1–4, 19–22).

Kedem-Katchalsky Flux Equations

An alternative, widely used set of flux equations is that derived by Kedem and Katchalsky (23), who began their analysis with an expression for the dissipation function per unit area of membrane obtained by formally integrating Eq. 1 across a membrane of uniform thickness. Assuming the volume fraction of permeant solute to be small (dilute solution approximation), they transformed the driving forces from transmembrane chemical potential differences for water and solute to differences in pressure and solute concentration in the solutions bathing the membrane. For the particular case in which the osmotic contribution of the permeant solute to volume flow is negligible, the Kedem-Katchalsky flux equations are:[1]

[1] When the osmotic pressure of the permeant solute ($RT\Delta C_S$) is not negligible, Eq. 5 contains an additional term (23): $J_v = k(\Delta P - \Delta\pi - \sigma^* RT\Delta C_S)$. There exists some doubt as to whether the Onsager reciprocity relations apply to these integrated flux equations, that is, whether or not the osmotic (σ^*) and con-

$$J_v = k(\Delta P - \Delta\pi), \tag{5}$$

$$J_s = \omega RT\Delta C_S + J_v(1 - \sigma)\overline{C}_S. \tag{6}$$

For definitions of symbols see List of Symbols.

Eq. 5 is analogous to Eq. 3, except that the hydraulic permeability (k) is regarded simply as a phenomenological coefficient. The diffusive and convective contributions to J_s in Eq. 6 are given by the terms involving ω and σ, respectively.

Solvent and Solute Mass Balances for the Glomerular Capillary Network

The expressions for transcapillary volume and solute fluxes (Eqs. 3 and 4 or Eqs. 5 and 6) may be combined with overall balances for volume and solute mass for the glomerular capillary network to obtain results in terms of measurable quantities. Following the analysis of Deen et al. (6), the glomerular capillary network is treated as a single tube of equivalent total surface area S and length L (Fig. 2). This approach assumes that radial concentration gradients within a glomerular capillary may be neglected, an approximation which has recently been confirmed to be valid (7). J_v and J_s are taken to be positive for transport from the glomerular capillary to Bowman's space, the latter assumed to be a well-mixed compartment having solute concentration C_{SB}. Of importance, J_v, J_s, the glomerular capillary plasma flow rate (Q), and the intracapillary protein and permeant solute concentrations (C_P and C_S, respectively) are all functions of the axial distance coordinate, x. The volume, protein, and solute balance equations are given by:

$$dQ/dx = -(S/L)J_v(x), \tag{7}$$

$$d(QC_P)/dx = 0, \tag{8}$$

$$d(QC_S)/dx = -(S/L)J_s(x). \tag{9}$$

As shown by Eq. 7, the rate of change of plasma flow along the idealized capillary is balanced by the volume flux, J_v, across the capillary wall. Eq. 8 states that the capillary wall is essentially impermeable to the major plasma proteins, while Eq. 9 represents the balance between changes in the mass flow of the permeable species along the capillary and the local net transcapillary solute flux, J_s.

Overall Transport Equations

The final transport equations based on either set of flux relations are obtained by substituting the appropriate expressions for J_v and J_s in Eqs. 7 and 9, and transforming the resulting equations using the following dimensionless variables:

$$\theta_S = C_S/C_{SA}, \tag{10}$$

vective (σ) reflection coefficients are equal (24). Because of the assumption that $RT\Delta C_S \ll \Delta P$, $\Delta\pi$, a condition fulfilled in the companion study (5), volume flow is independent of the permeant solute and only σ needs to be considered.

$$\theta_P = C_P/C_{PA} \tag{11}$$

$$\theta_{SB} = C_{SB}/C_{SA}, \tag{12}$$

$$\zeta = x/L. \tag{13}$$

The combined form of Eqs. 7 and 8 for either pore theory or the Kedem-Katchalsky approach is:

$$d\theta_P/d\zeta = F\theta_P^2[1 - A_1\theta_P - A_2\theta_P^2], \qquad \theta_P(0) = 1, \tag{14}$$

where the dimensionless parameters are:

$$F = K_f\overline{\Delta P}/Q_A, \tag{15}$$

$$A_1 = a_1 C_{PA}/\overline{\Delta P}, \tag{16}$$

$$A_2 = a_2 C_{PA}^2/\overline{\Delta P}. \tag{17}$$

Eq. 14, which has been discussed in detail previously (6), assumes that the transmembrane hydraulic pressure difference (ΔP) is constant along a glomerular capillary (i.e., $\Delta P = \overline{\Delta P}$), a good approximation for the rat (9). The colloid osmotic pressure difference ($\Delta\pi$) at any point along a capillary is related to C_P:

$$\Delta\pi = a_1 C_P + a_2 C_P^2, \tag{18}$$

where a_1 and a_2 are empirical coefficients (6). The glomerular ultrafiltration coefficient, K_f, a measurable quantity (11, 14–16), is related to the hydraulic permeabilities as follows:

$$K_f = kS = k'S' = (S'/l)(r_o^2/8\eta). \tag{19}$$

Thus, for pore theory, only two of the parameters K_f, S'/l, and r_o are independent. In addition to K_f, the other quantities in Eqs. 15–17 have also been measured under a variety of experimental conditions (8–16).

According to pore theory, the solute mass balance (Eq. 9) becomes:

$$\frac{d\theta_S}{d\zeta} = \frac{\theta_S}{\theta_P}\frac{d\theta_P}{d\zeta}\left\{1 - \frac{\chi_o(1 - (\theta_{SB}/\theta_S)\exp(-\gamma))}{1 - \exp(-\gamma)}\right\}, \qquad \theta_S(0) = 1. \tag{20}$$

For the Kedem-Katchalsky relations, the result is:

$$d\theta_S/d\zeta = -B\theta_P[\theta_S - \theta_{SB}] - (1/\theta_P)(d\theta_P/d\zeta)\{(1 - \sigma)\bar{\theta}_S - \theta_S\}, \qquad \theta_S(0) = 1 \tag{21}$$

where:

$$B = S\omega RT/Q_A. \tag{22}$$

The only additional expression required is one relating θ_{SB} to the transcapillary volume and solute fluxes:

$$\theta_{SB} = (1/C_{SA}) \int_0^1 J_s d\zeta \Big/ \int_0^1 J_v d\zeta. \tag{23}$$

Eq. 23 applies to Eq. 20 when J_v and J_s are evaluated using pore theory (Eqs. 3 and 4) and to Eq. 21 when the Kedem-Katchalsky relations (Eqs. 5 and 6) are used.

RESULTS

Predictions Based on Pore Theory

According to the pore theory outlined above, the transport of macromolecular solutes across the wall of the glomerular capillary will be determined by any two of the following membrane[2] parameters, S'/l, r_o, or K_f. Numerical solution of Eqs. 14 and 20 provides insight into how the transcapillary driving forces and membrane parameters interact in theory to influence the fractional clearance, θ_{SB}, of a partially permeable macromolecule. Examples are shown in Fig. 3. Using values of $\overline{\Delta P}$, π_A, and K_f representative of the normal Wistar rat (Table I), θ_{SB} is plotted as a function of the

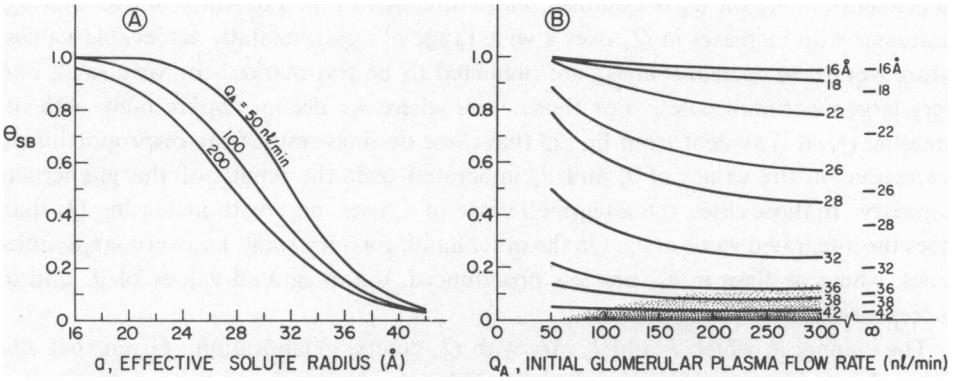

FIGURE 3 Relationship between fractional solute clearance (θ_{SB}), effective solute radius, and Q_A. Values for C_{PA}, K_f, and $\overline{\Delta P}$ are as given in Table I and r_o = 50 Å. The shaded area at the bottom of Fig. 3 B denotes the region where transcapillary solute exchange is governed solely by convection. In the limit $Q_A \to \infty$, $\theta_{SB} = \chi_o\psi$ as shown on the right-hand side of Fig. 3 B.

[2]The glomerular capillary wall is actually a highly complex composite of several distinct anatomical structures. The word "membrane" is used here to refer to the functional properties of this composite and is not to be confused with any specific anatomical structure, such as the glomerular capillary basement membrane.

TABLE I

PHYSIOLOGICAL QUANTITIES AND MEMBRANE PARAMETERS DEFINING THE REFERENCE STATE FOR THE NORMAL WISTAR RAT

$\overline{\Delta P}$	= 35.3 mm Hg
C_{PA}	= 5.8 g/100 ml
π_A	= 19.2 mm Hg
Q_A	= 65.0 nl/min
K_f	= 0.08 nl/(s·mm Hg)

Values taken from refs. 9 and 11.

Stokes-Einstein solute radius, a (Fig. 3 A), and as a function of initial glomerular plasma flow rate, Q_A (Fig. 3 B), a quantity that may easily be varied experimentally over the range shown. The pore radius, r_o, has been assumed to equal 50 Å, a value calculated by others from fractional solute clearance profiles measured in man and experimental animals, using hydrodynamic theories of transport through isoporous membranes (1, 3, 4, 19, 25, 26).

With this value of r_o = 50 Å, the predicted fractional clearance profiles shown in Fig. 3 A are remarkably similar to profiles obtained in experimental studies using polyvinylpyrrolidone (PVP) and dextrans as test solutes (1, 3, 4, 19, 25, 26). It is clear from Fig. 3 A that fractional solute clearance profiles (the relationship between θ_{SB} and a, the effective solute radius) cannot be taken to reflect the permselective properties of the glomerular capillary wall alone, since values of θ_{SB} are predicted to vary markedly with alterations in Q_A, one of the major determinants of SNGFR (6, 9). This predicted dependence of θ_{SB} on Q_A is examined more directly in Fig. 3 B, which shows that θ_{SB} decreases with increases in Q_A over a wide range of experimentally achievable values. Moreover, these decreases in θ_{SB} are predicted to be less marked for very small and very large macromolecules. For those cases where θ_{SB} declines appreciably with increasing Q_A, it is evident from Eq. 23 that these declines result from disproportionate alterations in the values of J_s and J_v integrated over the length of the glomerular capillary. In those cases, the integrated value of J_v rises more with increasing Q_A than does the integrated value of J_s. On the other hand, for very small and very large molecules, where declines in θ_{SB} are less pronounced, the integrated values of J_s and J_v increase roughly in proportion.

The manner in which J_v and J_s vary with Q_A deserves elaboration. Given that single nephron glomerular filtration rate, SNGFR, is proportional to the denominator in Eq. 23:

$$\text{SNGFR} = S \cdot \int_0^1 J_v d\zeta, \tag{24}$$

and since SNGFR has been shown to be highly plasma-flow dependent (9), it would be expected that θ_{SB} would also be sensitive to changes in Q_A. The dependence of water transport on Q_A is not sufficient, however, to account for the trends seen in

Fig. 3 B, since the absolute rate of solute transport, proportional to the numerator in Eq. 23, is also flow-dependent. An examination of the dependence of J_s on Q_A requires an assessment of the relative contributions of convection and diffusion to transcapillary solute exchange. As the first step, Eq. 4 is substituted into Eq. 23, yielding:

$$\theta_{SB}/\chi_o = \int_0^1 \theta_S J_v \psi \, d\zeta \Big/ \int_0^1 J_v \, d\zeta, \tag{25}$$

where:

$$\psi(\zeta) = [1 - \beta \exp(-\gamma)]/[1 - \exp(-\gamma)], \tag{26}$$

and:

$$\beta(\zeta) = \theta_{SB}/\theta_S. \tag{27}$$

The quantity $\gamma(\zeta)$ is a measure of the relative importance of convection ($\chi_o J_v$) and diffusion ($\xi_o \mathfrak{D}_s / l$) to solute transport within a pore at any point ζ along an idealized glomerular capillary. The significance of the function $\psi(\zeta)$ in Eq. 25 is that it is the sole determinant of the relative effects of convection and diffusion on θ_{SB}. This can be seen by noting in Eq. 26 that as γ becomes large and convection is totally dominant, $\psi \rightarrow 1$. If, in the derivation of Eq. 4 (see Appendix), the diffusion term is eliminated, θ_{SB}/χ_o is given by Eq. 25 with $\psi \equiv 1$, thereby confirming that convection will be the sole mechanism for solute transport whenever $\psi = 1$. As shown in Fig. 4, this is the case when $\gamma > 3$. For lower values of γ, where $\psi > 1$, convection and diffusion both contribute to the transcapillary exchange of solute.[3]

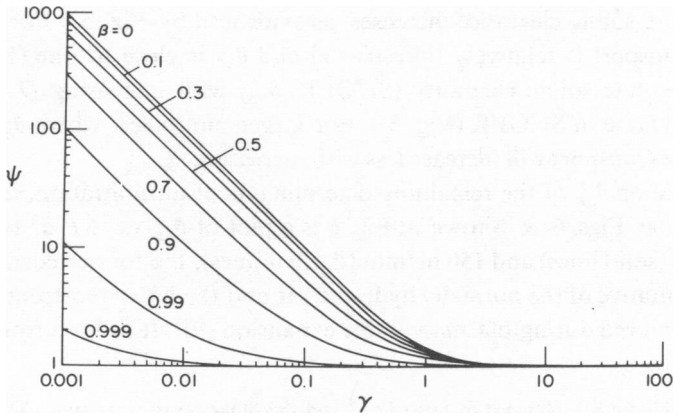

FIGURE 4 Relationship between ψ and γ for $0 \leq \beta \leq 1$.

[3] This statement is true only if $\beta < 1$. According to pore theory, however, the case $\beta = 1$ is not permissible, since pore theory predicts that some restriction to solute exchange must occur for all solute sizes.

For a given solute, γ is not constant along a glomerular capillary, but rather decreases as J_v decreases.[4] Thus diffusion tends to be less important at the afferent ($\zeta = 0$) than at the efferent ($\zeta = 1$) end of the capillary, the magnitude of this effect depending on the range of γ. When the minimum value of γ (γ_{min}, attained at $\zeta = 1$) exceeds ~3, transcapillary exchange for the given solute will be governed solely by convection. The shaded region in Fig. 3 B denotes the range of molecular sizes and glomerular plasma flow rates where this is the case. Alternatively, when the maximum value of γ (γ_{max}, attained at $\zeta = 0$) does not exceed ~3, convection and diffusion both contribute to solute transport along the entire length of the capillary, as predicted for $a < 36$ Å and $Q_A < 300$ nl/min in Fig. 3 B. Finally, when $\gamma_{max} > 3$ and $\gamma_{min} < 3$, convection will dominate transcapillary solute exchange at the afferent end of the capillary, whereas diffusion as well as convection will contribute nearer the efferent end.

Increases in Q_A have the effect of elevating J_v at any point along a glomerular capillary (6); hence γ increases with Q_A. If initially $\gamma < 3$, changes in γ will result in changes in ψ (Fig. 4) and θ_{SB} (Eq. 25). The greatest flow dependence of θ_{SB} occurs when variations in ψ are greatest, that is, when $\gamma_{max} < 3$, corresponding to low values of Q_A. Almost no flow dependence of θ_{SB} is evident when $\gamma_{min} > 3$, a situation favored by high values of Q_A. Hence, in Fig. 3 B, the flow dependence of θ_{SB} diminishes progressively at higher values of Q_A. As Q_A increases without limit, $\theta_{SB} \rightarrow \chi_o\psi$. This lower bound for θ_{SB} (values of which are given on the right-hand margin of Fig. 3 B), restricts the plasma-flow dependency for small molecules ($a <$ ~20 Å) more than that for middle-sized molecules (~20 Å $< a <$ ~34 Å). For any size molecule, for large enough values of Q_A, solute transport will be governed only by convection and θ_{SB} will approach the limiting value of $\chi_o\psi$.

It is important to recognize that despite the fact that θ_{SB} declines with increases in Q_A, the absolute solute clearance increases, as evidenced by Fig. 5. For small molecules, since transport is relatively unrestricted and θ_{SB} is close to one (Fig. 3 B), the increase in absolute solute clearance (SNGFR $\cdot \theta_{SB}$) with increasing Q_A will closely parallel the increase in SNGFR (Fig. 5). For larger molecules, where θ_{SB} is smaller, absolute solute transport will increase less with increasing Q_A.

The influence on θ_{SB} of the remaining determinants of ultrafiltration, $\overline{\Delta P}$, C_{P_A}, and K_f, is examined in Figs. 6–8. Shown in Fig. 6 is a plot of θ_{SB} vs. $\overline{\Delta P}$ at two values of Q_A, 65 nl/min (solid lines) and 150 nl/min (dashed lines), the former corresponding to values representative of the normally hydrated rat and the latter representing a typical value of Q_A achieved during plasma volume expansion (9). It follows from the defini-

[4] An explicit formula for γ is obtained by using Eq. 3 and the Stokes-Einstein relation, $\mathfrak{D}_\infty = kT/6\Pi\eta a$. Assuming $r_o = 50$ Å: $\gamma \equiv \chi_o J_v' l/\xi_o \mathfrak{D}_\infty = (1.85 \times 10^{-4})(\chi_o/\xi_o)\, a(\overline{\Delta P} - \Delta\pi)$, where a is in angstroms and $\overline{\Delta P}$ and $\Delta\pi$ are in millimeters of Hg. In this expression, the only quantity that varies along a glomerular capillary is $\Delta\pi$, which in the rat typically increases from some 19 mm Hg at the afferent end to 35 mm Hg at the efferent end (9). High values of Q_A reduce the extent of this rise in $\Delta\pi$ along the capillary (11). At extremely high values of Q_A, $\Delta\pi \rightarrow \pi_A$ everywhere along the capillary, so that γ achieves its maximum value, γ_{max}, in pores everywhere along the capillary.

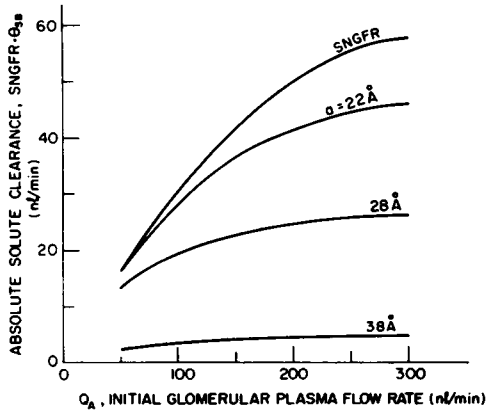

FIGURE 5

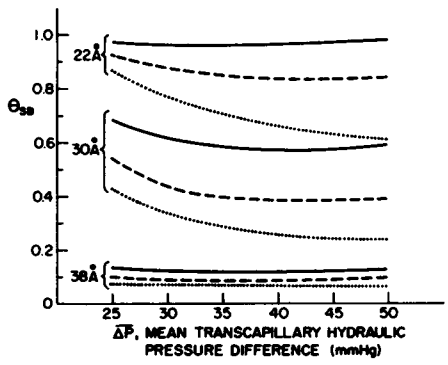

FIGURE 6

FIGURE 5 Relationship between absolute solute clearance (SNGFR·θ_{SB}) and initial glomerular plasma flow rate (Q_A) for three representative values of the effective solute radius (a).

FIGURE 6 Relationship between fractional solute clearance (θ_{SB}) and mean glomerular transcapillary hydraulic pressure difference ($\overline{\Delta P}$) for three representative values of the effective solute radius. Solid and dashed lines correspond to values of Q_A = 65 and 150 nl/min, respectively. Dotted lines represent the limiting values reached as $Q_A \rightarrow \infty$.

tion of γ that increases in $\overline{\Delta P}$ (which elevate J_v) cause increases in γ_{max} and to some extent increases in γ_{min}. As a result, θ_{SB} would be expected to be increasingly insensitive to changes in $\overline{\Delta P}$ as $\overline{\Delta P}$ is increased, since ψ changes less at these higher values of γ (Fig. 4). Hence, θ_{SB} in Fig. 6 is relatively constant at high values of $\overline{\Delta P}$, as was the finding for high values of Q_A. The effects of C_{PA} (or π_A) on θ_{SB}, shown in Fig. 7, are essentially the same as those of inverse changes in $\overline{\Delta P}$, since C_{PA} (or π_A) and $\overline{\Delta P}$ affect γ in an opposite manner. The dotted lines in Figs. 6 and 7 represent values of $\chi_o\psi$, the lower limit for θ_{SB} achieved at extremely high values of Q_A.

As shown in Fig. 8, decreases in K_f lead to decreases in θ_{SB}. As K_f declines to very small values, $\Delta\pi$, γ, and ψ become essentially constant along the length of the capillary. Under these conditions, θ_{SB} approaches the same lower limit as found previously for large values of Q_A, namely, $\chi_o\psi$ (shown again by the dotted lines in Fig. 8). If $\gamma > \sim 3$, which is the case for molecular radii exceeding ~ 34 Å, $\psi \simeq 1$ for very low K_f and convection is the only mechanism for solute transport. For molecules smaller than ~ 34 Å, both convection and diffusion will contribute to solute transport in spite of the low value of K_f. On the other hand, as K_f increases, $\Delta\pi$ rises more rapidly along the capillary (6), and γ_{min} is reached at a more afferent point. Hence, diffusion of solute becomes increasingly more important and θ_{SB} rises progressively with increases in K_f.

Predictions Based on the Kedem-Katchalsky Equations

Using the flux relations derived by Kedem and Katchalsky (23), the glomerular transcapillary exchange of a partially permeable solute is governed by three membrane

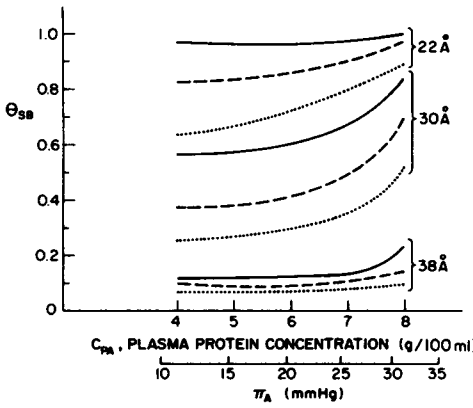

FIGURE 7

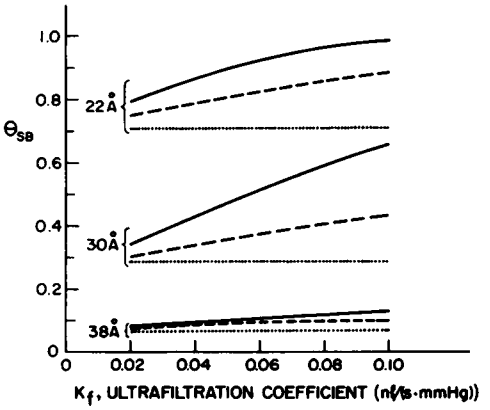

FIGURE 8

FIGURE 7 Dependence of θ_{SB} on C_{PA} (or π_A) for three different size molecules. Solid, dashed, and dotted lines are as given in Fig. 6.

FIGURE 8 Dependence of θ_{SB} on K_f, the glomerular capillary ultrafiltration coefficient. Solid, dashed, and dotted lines are as given in Fig. 6. In these calculations, K_f was varied by changing S'/l, with r_o held constant.

parameters, ωS, σ, and K_f. Closely following the approach given for pore theory, numerical solution of Eqs. 14 and 21 allows calculation of how the fractional solute clearance, θ_{SB}, of a partially permeable macromolecule varies with selected alterations in the transcapillary driving forces and membrane parameters.

Using values of $\overline{\Delta P}$, π_A, and K_f representative of the normal Wistar rat (Table I), θ_{SB} is plotted in Fig. 9 as a function of initial glomerular plasma flow rate, Q_A, for

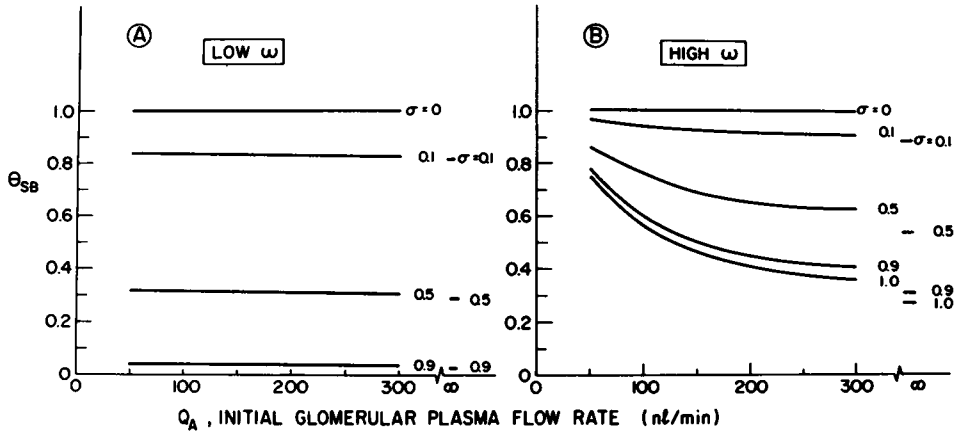

FIGURE 9 Dependence of fractional solute clearance (θ_{SB}) on Q_A for various assumed values of the solute reflection coefficient (σ) and low and high values of the solute permeability (ω). Low and high values of ω are 10^{-17} and 10^{-14} mol/(dyn·s), respectively. S is assumed to be 0.0019 cm^2 (28); hence $S\omega RT$ for Figs. 9 A and 9 B is 0.0284 and 28.4 nl/min, respectively. Values for C_{PA}, K_f, and $\overline{\Delta P}$ are as given in Table I.

low and high values of the solute permeability, ω, and for $0 \leq \sigma \leq 1$. These low and high values of ω correspond roughly to the experimentally measured bounds for this parameter for a wide range of synthetic and biological membranes (27). For a low value of ω (Fig. 9 A) θ_{SB} is essentially independent of changes in Q_A over the range examined. In contrast, when ω is high (Fig. 9 B), θ_{SB} decreases with increasing Q_A for $\sigma > 0$. Furthermore, when ω is large, θ_{SB} is always larger for any given value of Q_A than when ω is small. As will soon be discussed, this is so because solute transport by diffusion has been added to that by bulk flow.

These theoretical results may best be explained in the following manner. Combining Eqs. 6 and 23 gives:

$$\theta_{SB} = \left[S\omega RT \int_0^1 (1 - \beta)\theta_S d\zeta \Big/ \text{SNGFR}\right] + (1 - \sigma)\left(\int_0^1 J_v \bar{\theta}_S d\zeta \Big/ \int_0^1 J_v d\zeta\right). \quad (28)$$

Unlike the equivalent expression derived for pore theory (Eq. 25), Eq. 28 has readily distinguishable terms representing diffusion (dependent on ω) and convection (dependent on σ). From this equation it is evident that for $\sigma \neq 1$ convection will be the dominant mode of solute transport provided ω is made sufficiently small. Such is the case for the predictions shown in Fig. 9 A which indicate that whenever convection is the primary mechanism governing transcapillary solute exchange, θ_{SB} will be insensitive to changes in Q_A. When ω is large (Fig. 9 B) diffusional processes become more important and therefore θ_{SB} is larger for given values of Q_A and σ than in Fig. 9 A, since the effects of diffusion and convection are additive (Eq. 28). As $\sigma \rightarrow 1$ diffusion becomes increasingly important, and when $\sigma = 1$, diffusion becomes the sole means for solute transport. In contrast to this, when $\sigma \rightarrow 0$, convection of solute becomes increasingly more important, and when $\sigma = 0$, convection becomes the sole means for solute transport for any value of ω since in this case $\beta = 1$.

In the limit of very high glomerular plasma flow rates, $\theta_S \rightarrow 1$ and θ_{SB} reaches a minimum value, $(\theta_{SB})_{\min}$, given by:

$$(\theta_{SB})_{\min} = \frac{S\omega RT[1 - (\theta_{SB})_{\min}]}{K_f(\overline{\Delta P} - \pi_A)} + (1 - \sigma)\frac{1 - (\theta_{SB})_{\min}}{\ln[1/(\theta_{SB})_{\min}]}. \quad (29)$$

A useful approximation to Eq. 29 is given by:

$$(\theta_{SB})_{\min} \simeq \frac{S\omega RT + [(1 - \sigma)/2]K_f(\overline{\Delta P} - \pi_A)}{S\omega RT + [(1 + \sigma)/2]K_f(\overline{\Delta P} - \pi_A)}. \quad (30)$$

Values of $(\theta_{SB})_{\min}$ computed from Eq. 29 are shown on the right-hand margins of Figs. 9 A and 9 B. As can be seen more clearly from Eq. 30, $\theta_{SB} = (\theta_{SB})_{\min} = 1$ for $\sigma = 0$, irrespective of the values of ω or the other quantities in Eq. 30. For solute

transport only by convection ($\omega = 0$), $(\theta_{SB})_{min} \simeq (1 - \sigma)/(1 + \sigma)$, an expression which gives values of $(\theta_{SB})_{min}$ essentially equivalent to those shown in Fig. 9 A. In contrast, when ω is large (Fig. 9 B), $(\theta_{SB})_{min}$ is determined by diffusion as well as by convection of solute (Eq. 30). Consequently, constancy of θ_{SB} at high values of Q_A does not imply that solute transport is dominated by convection. If, however, convection is essentially the sole mechanism for solute transport, as when ω is small (Fig. 9 A), θ_{SB} will be relatively constant.

The results given in Fig. 9 are in general agreement with the plasma flow dependence of θ_{SB} obtained using pore theory. As shown in Fig. 9 B, θ_{SB} is most sensitive to changes in Q_A at low values of Q_A, where diffusional processes contribute maximally. This same behavior was found using pore theory, as evidenced by the low-flow region in Fig. 3 B. Since θ_{SB} is bounded below by the value of $(\theta_{SB})_{min}$ computed from Eq. 29, it is not possible for significant flow dependence to exist when σ is small (i.e., $\sigma < \sim 0.1$). However, as $\sigma \rightarrow 1$, corresponding to molecules with larger radii, significant flow dependence is predicted (Fig. 9 B), a result in apparent contradiction with that obtained using pore theory (Fig. 3 B). This discrepancy arises since the effective diffusivity employed in the pore model varies inversely with the solute radius, whereas nonequilibrium thermodynamics permits σ and ω to vary independently of one another, and ω in Fig. 9 was arbitrarily chosen to be the same for each value of σ. Although ω would also be expected to vary inversely with the solute radius, this may not be the case if there are chemical interactions between solute and membrane.

Fig. 10 shows that the absolute solute clearance is an increasing function of Q_A, for either low or high ω. As $\sigma \rightarrow 0$, increases in solute clearance closely parallel increases in SNGFR, also predicted for small molecules from pore theory (Fig. 5). Comparison of Fig. 10 A (low ω) with Fig. 10 B (high ω) clearly demonstrates the potentially important contribution of diffusion to the absolute rate of solute transport. Changes in solute clearance follow changes in SNGFR less closely as $\sigma \rightarrow 1$.

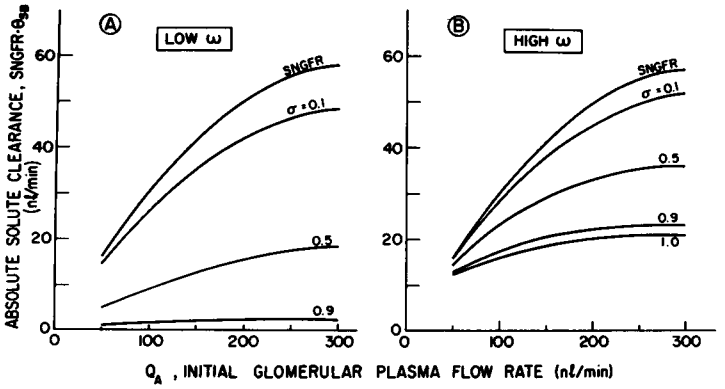

FIGURE 10 Relationship between absolute solute clearance (SNGFR·θ_{SB}) and initial glomerular plasma flow rate (Q_A) for various values of the reflection coefficient (σ), and for the same low and high values of the solute permeability (ω) as given in Fig. 9.

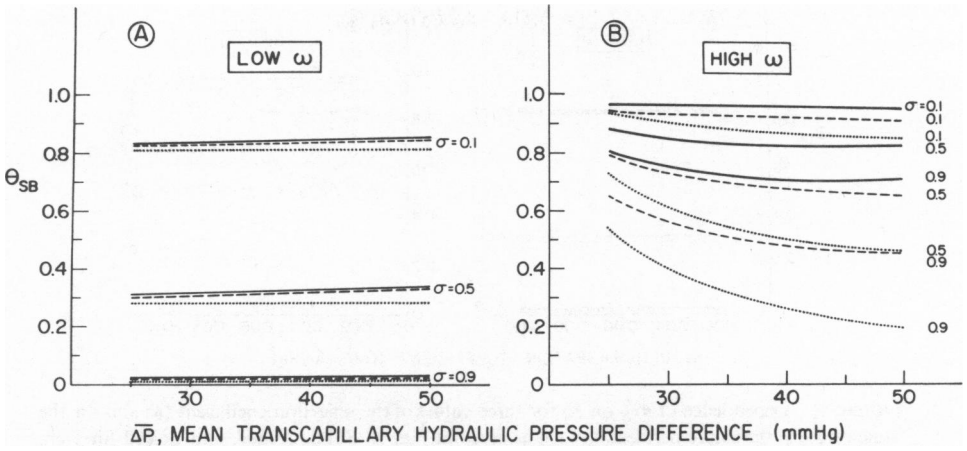

FIGURE 11 Dependence of θ_{SB} on $\overline{\Delta P}$ for three values of the reflection coefficient (σ) and for the same values of the solute permeability (ω) as given in Fig. 9. Solid, dashed, and dotted lines correspond to Q_A = 65 nl/min, Q_A = 150 nl/min, and $Q_A \to \infty$, respectively.

The effects on θ_{SB} of variations in the other determinants of ultrafiltration, $\overline{\Delta P}$, C_{PA}, and K_f, are shown in Figs. 11–13. In Figs. 11 A and 11 B, θ_{SB} is plotted as a function of $\overline{\Delta P}$ at two values of Q_A, 65 nl/min and 150 nl/min. Since J_v changes in parallel with changes in $\overline{\Delta P}$, diffusion would be expected to become the important mode of solute transport as $\overline{\Delta P}$ decreases (approaching π_A), whereas convective solute transport becomes increasingly more important as $\overline{\Delta P}$ rises. In Fig. 11 A, where

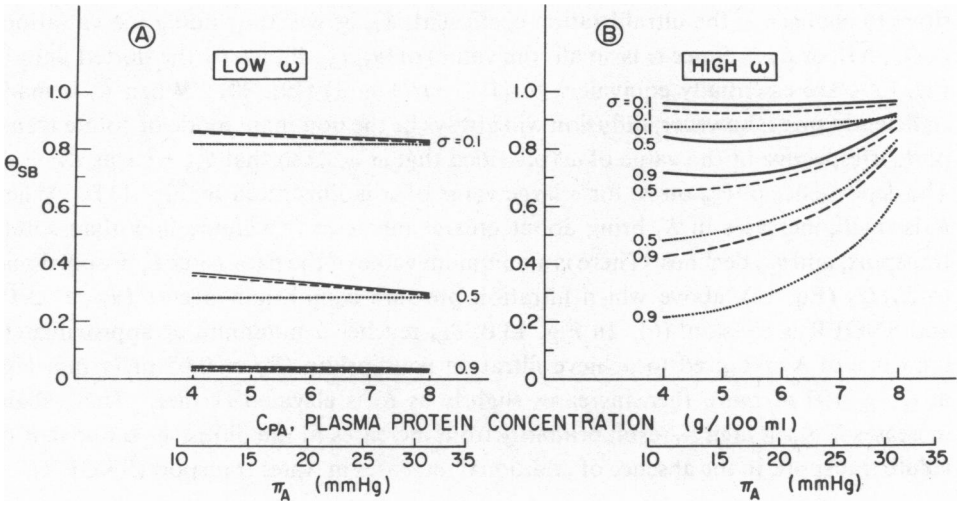

FIGURE 12 Dependence of θ_{SB} on C_{PA} (or π_A) for three values of the reflection coefficient (σ) and for the same values of the solute permeability (ω) as given in Fig. 9. Solid, dashed, and dotted lines are as given in Fig. 11.

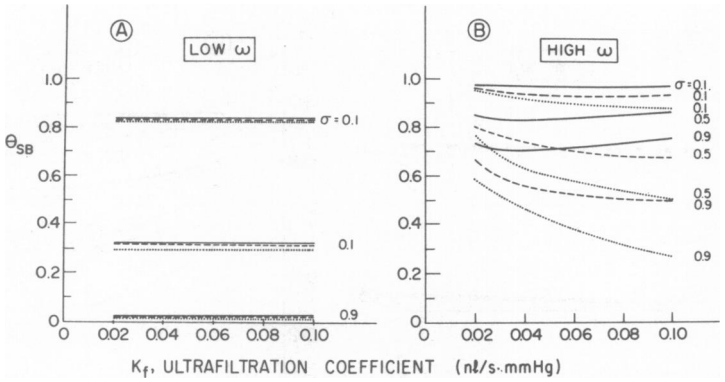

FIGURE 13 Dependence of θ_{SB} on K_f for three values of the reflection coefficient (σ) and for the same values of the solute permeability (ω) as given in Fig. 9. Solid, dashed, and dotted lines are as given in Fig. 11.

diffusion is essentially absent, θ_{SB} is insensitive to alterations in $\overline{\Delta P}$ over the range examined. The fact that θ_{SB} increases slightly as $\overline{\Delta P}$ increases follows from small increases in $\bar{\theta}_S$ in the convective term of Eq. 28. When ω is large, however, as in Fig. 11 B, the diffusive term in Eq. 28 is no longer negligible and θ_{SB} falls significantly with increases in $\overline{\Delta P}$. This dependence of θ_{SB} on $\overline{\Delta P}$ is qualitatively similar to that shown in Fig. 6 for pore theory. As was the case for pore theory, changes in C_{PA} (or π_A) are largely equivalent to inverse changes in $\overline{\Delta P}$. This dependence of θ_{SB} on C_{PA} (or π_A) is illustrated in Fig. 12. In addition, the dotted lines in Figs. 11 and 12 represent the lower limits of θ_{SB} achieved at very high values of Q_A (Eq. 29).

Fig. 13 A shows that when ω is small and diffusion is unimportant, θ_{SB} remains insensitive to changes in the ultrafiltration coefficient, K_f, as was the finding for variations in Q_A, $\overline{\Delta P}$, or C_{PA}. Since ω is small, the values of $(\theta_{SB})_{min}$ shown by the dotted lines in Fig. 13 A are essentially equivalent to $(1 - \sigma)/(1 + \sigma)$ (Eq. 30). When K_f is made sufficiently small, however, diffusion will always be the dominant mode of solute transport, irrespective of the value of ω (provided that $\omega \neq 0$) so that $\theta_{SB} \rightarrow 1$ as $K_f \rightarrow 0$. The dependence of θ_{SB} on K_f for a large value of ω is illustrated in Fig. 13 B. When K_f is small, increases in K_f bring about greater increases in volume flow than solute transport, and θ_{SB} declines. There is a minimum value of the parameter F, proportional to K_f/Q_A (Eq. 15), above which filtration pressure equilibrium occurs ($\pi_E \simeq \overline{\Delta P}$) and SNGFR is constant (6). In Fig. 13 B, θ_{SB} reaches a minimum at approximately the value of K_f required to achieve filtration equilibrium ($K_f \simeq 0.05$ nl/(s·mm Hg) at $Q_A = 150$ nl/min), then increases slightly as K_f is elevated further. These slight increases in θ_{SB} at high K_f result primarily from increases in the diffusive component of solute transport, in the absence of additional increases in water transport (SNGFR).

DISCUSSION

We have examined two alternate theoretical approaches for characterizing the permselective properties of the glomerular capillary wall. In so doing, we have discussed in

some detail the predicted influences of variations in the determinants of glomerular filtration rate, namely, Q_A, $\overline{\Delta P}$, C_{P_A}, and K_f, on fractional solute clearance. Overall, the results obtained using pore theory and the Kedem-Katchalsky equations are in good qualitative agreement. A particularly important result, in keeping with the findings of other workers (1–4), is that fractional solute clearance is strongly dependent on the determinants of glomerular filtration rate when convection and diffusion both contribute to solute exchange. When convection becomes the sole mechanism for transcapillary solute exchange, however, fractional solute clearance is essentially independent of changes in the determinants of glomerular filtration rate. Thus, whenever diffusion plays an important role, experimental values of fractional solute clearance would be expected to depend on the values of Q_A, $\overline{\Delta P}$, C_{P_A}, and K_f. Consequently, fractional clearance profiles alone are insufficient to characterize the permselective properties of the glomerular capillary wall, since alterations in these profiles due to disease or following an experimental maneuver may reflect changes in glomerular pressures and flows as well as changes in the properties of the capillary wall per se.

It has long been recognized that there tends to be an inverse dependence of filtrate solute concentration on filtration rate through restrictive membranes, and explicit equations have been derived previously (1–4) which, when applied to a single glomerulus, may be used to relate θ_{SB} and SNGFR. Pappenheimer (1) and Renkin (2) proposed the following relationship:

$$\theta_{SB} = C_{SB}/C_{SA} = (k_1 \text{SNGFR} + k_2)/(\text{SNGFR} + k_2), \tag{31}$$

where k_1 and k_2 are constants related to solute diffusivity and pore geometry (1–3). Eq. 31 assumes that convective transport of solute is proportional to C_{SA}, but Verniory et al. (4) correctly pointed out that it is more appropriate to treat convective transport as proportional to an integrated mean concentration within a pore, and obtained the following result:

$$\theta_{SB} = k_3/[1 - (1 - k_3)\exp(-k_4 \text{SNGFR})], \tag{32}$$

where k_3 and k_4 are again constants related to solute diffusivity and pore geometry (4). It is instructive to note that Eqs. 31 and 32, despite their differences, both predict an inverse dependence of θ_{SB} on SNGFR, with $\theta_{SB} \rightarrow 1$ as SNGFR $\rightarrow 0$ and $\theta_{SB} \rightarrow k_1$ or k_3 (where $k_1, k_3 < 1$) as SNGFR $\rightarrow \infty$. Since SNGFR increases with increasing initial glomerular plasma flow rate, Q_A (see Fig. 5, for example), the predictions of Eqs. 31 and 32 are in good qualitative agreement with the dependence of θ_{SB} on Q_A shown in Figs. 3 and 9 B. Furthermore, if diffusion is negligible, $k_2 \rightarrow 0$ (1–3) and $k_4 \rightarrow \infty$ (4), in which case θ_{SB} is indicated by Eqs. 31 and 32 to be insensitive to SNGFR, corresponding to our results for small ω (see Fig. 9 A, for example).

The results of the present study are based on overall mass balance equations (Eqs. 7–9) which allow realistic variations in J_s and J_v along a glomerular capillary, whereas the application of Eqs. 31 and 32 requires J_s and J_v to be uniform along a capillary (1–4). It is therefore not surprising that Eqs. 31 and 32, while often qualitatively cor-

rect, nonetheless fail in several instances to predict the proper relationship between changes in SNGFR and θ_{SB}. For example, it can be seen in Figs. 6 and 11 B that for a value of Q_A typical of the normal hydropenic rat (65 nl/min), increases in $\overline{\Delta P}$ from 35 to 50 mm Hg have essentially no effect on θ_{SB}, although this increase in $\overline{\Delta P}$ results in approximately a 40% increase in SNGFR. In contrast, the same 40% increase in SNGFR, caused by elevating Q_A from 65 to 90 nl/min with $\overline{\Delta P}$ held constant at 35 mm Hg, is shown by Figs. 3 and 9 B to cause appreciable reductions in θ_{SB}. Thus, it can be concluded that the effects on θ_{SB} of changes in the various determinants of SNGFR do not result simply from changes in SNGFR alone, but instead reflect a coupling of the variations in J_v and J_s taking place along the capillary. Since previous studies (1–4) have neglected these variations, the present approach offers a clear advantage in the ability to predict the effects on θ_{SB} of variations in glomerular pressures and flows. Consequently, use of the present formulation in computing membrane parameters from experimental measurements will result in values that more nearly reflect the permselective properties of the glomerular capillary wall.

Unfortunately, it is not possible to provide a quantitative comparison of the predictions obtained using the two sets of flux equations employed in the present study unless the membrane parameters for solute transport obtained from the Kedem-Katchalsky equations, ω and σ, are related to specific frictional interactions among the solute, solvent, and membrane. Although such a frictional representation of ω and σ is available (27), it requires that additional assumptions be made and thereby results in a less general description of membrane transport. Anderson and Quinn (22) attempted to compare pore theory and the Kedem-Katchalsky equations in this way, but these workers assumed that solute-solvent frictional interactions within the membrane were equivalent to those in free solution, which seems unlikely.

Although there is good qualitative agreement between these two descriptions of membrane transport, an important fundamental distinction sets them apart. With pore theory it is necessary to assume for the membrane phase a particular geometric structure (i.e. cylindrical pores), whereas the internal structure of the membrane need not be specified in deriving the Kedem-Katchalsky flux relations. The structural complexity of biological membranes makes it unlikely that the exact hydrodynamic conditions required by pore theory are ever achieved in a biological system. Nonetheless, estimation of membrane parameters based on pore theory might still yield useful insight into the special permselectivity characteristics which glomerular capillary walls are known to possess. A distinct advantage of pore theory is that it is easier to use in computing membrane parameters from experimental data, since K_f, S'/l, and r_o are related by Eq. 19. Thus, for an isoporous membrane, there are only two independent parameters to be calculated (r_o and K_f or S'/l), whereas three parameters (K_f, ωS, and σ) are needed for the Kedem-Katchalsky approach.

Several attempts have been made to test pore theory using synthetic membranes and other porous materials. The data presently available fail to lend strong support for the expression for the ratio of solute diffusivity in the pore to that in free solution (ξ_o, Eq. 49); the expression for the sieving coefficient (χ_o, Eq. 50) has not been

tested because experiments reported thus far have been carried out in the absence of water transport. Uzelac and Cussler (29) and Satterfield et al. (30), for example, present data which are inconsistent with the steric exclusion term in the expression for ξ_o, a value of unity having been found for the steric term, theoretically equal to $(1 - \lambda)^2$, despite values of λ up to 0.5. The latter authors also point out that the experimental results of Beck and Schultz (31) using track-etched mica membranes, often cited as support for the expression for ξ_o, are equally consistent with a purely empirical exponential relationship between ξ_o and λ (30). In fact, since the values of λ used by Beck and Schultz (31) were generally less than 0.2, many different functions of λ would adequately describe their data. In a more recent study using track-etched polycarbonate membranes, Van Bruggen et al. (32) found large discrepancies between measured and calculated values of ξ_o for inulin, where λ was only 0.1. It would seem, therefore, that even for track-etched membranes, which are considered to be excellent representations of the idealized membranes referred to in pore theory, convincing experimental evidence for the validity of a hydrodynamic model of porous membrane transport is still lacking. It is difficult to subject the Kedem-Katchalsky equations to similarly rigorous tests, and their range of applicability likewise remains uncertain. Despite the various reservations concerning the application to biological membranes of these two sets of flux relations, it would appear that either approach can be usefully employed in characterizing the permselectivity of the glomerular capillary wall.

LIST OF SYMBOLS

a	Stokes-Einstein radius of solute molecule, $\hat{k}T/6\Pi\eta\mathfrak{D}_\infty$.
a_1, a_2	Empirical constants in Eq. 18, 1.629 mm Hg/(g/100 ml) and 0.2935 mm Hg/(g/100 ml)^2, respectively.
a_i	Activity of species i.
A	Cross-sectional area of pore, Πr_o^2.
A_1, A_2	Dimensionless osmotic pressure coefficients defined by Eqs. 16 and 17, respectively.
B	Dimensionless solute permeability and plasma flow rate parameter, defined by Eq. 22.
$\tilde{C}$	Total molar concentration.
$\tilde{C}_i$	Molar concentration of species i.
$\hat{C}_s(z)$	Mass solute concentration within a pore. At each end of the pore we assume $\hat{C}_s$ equals the bulk concentration of the solute on that side.
C_o, C_l	Mass solute concentration in bulk solutions at $z = 0$ and $z = l$, respectively.
$C_S(x), C_P(x)$	Mass concentrations of solute and plasma protein at any point along an idealized glomerular capillary.
C_{SA}, C_{PA}	Initial glomerular capillary (or afferent arteriolar) solute and plasma protein concentrations, respectively.
C_{SB}	Solute concentration in Bowman's space.
$\overline{C}_S(x)$	Log mean solute concentration at any point along an idealized glomerular capillary, $(C_S - C_{SB})/\ln(C_S/C_{SB})$.
$\Delta C_S(x)$	Transcapillary solute concentration difference at any point along an idealized glomerular capillary, $C_S - C_{SB}$.
d_i	Generalized mass transfer driving force for species i, defined by Eqs. 33 and 34.

$\mathfrak{D}_\infty$	Solute diffusivity in free solution.
D_{ij}	Multicomponent diffusivity for the species pair, i and j.
F	Dimensionless permeability and plasma flow rate parameter, defined by Eq. 15.
F_{sw}, f_{sm}, f_{wm}	Local frictional coefficients defined by Eq. 38.
$G(\lambda, \rho)$	Local lag coefficient between solute and water velocities.
J_s, J_s'	Transcapillary mass solute flux at any point along an idealized glomerular capillary, based on total membrane area and total pore area, respectively.
J_v, J_v'	Transcapillary volume flux at any point along an idealized glomerular capillary, based on total membrane area and total pore area, respectively.
k, k'	Effective hydraulic permeability of the capillary wall, based on total membrane area and total pore area, respectively.
k_1, k_2, k_3, k_4	Constants related to solute diffusivity and pore geometry, Eqs. 31 and 32.
$\hat{k}$	Boltzmann's constant.
K_f	Ultrafiltration coefficient, defined by Eq. 19.
$K(\lambda, \rho)$	Local ratio of bulk-to-pore solute diffusivity.
l	Pore length.
L	Length of idealized glomerular capillary.
$\tilde{N}$	Avogadro's number.
N_i	Molar flux of species i relative to the mass average velocity.
P	Pressure.
$\Delta P(x)$	The difference between hydraulic pressure at any point along an idealized glomerular capillary, and hydraulic pressure in Bowman's space.
$\overline{\Delta P}$	Length-averaged value of the glomerular transcapillary hydraulic pressure difference.
ΔP^+	Excess pressure drop in pore due to the solute.
$Q(x)$	Volumetric plasma flow rate at any point along an idealized glomerular capillary.
Q_A	Initial glomerular capillary (or afferent arteriolar) plasma flow rate.
r_o	Pore radius.
R	Universal gas constant.
R_{ij}	Hydrodynamic resistance coefficients, Eq. 43.
S, S'	Total membrane surface area and total pore area, respectively.
SNGFR	Single nephron glomerular filtration rate, Eq. 24.
T	Absolute temperature.
v	Mass average velocity.
v_i	Velocity of species i relative to stationary coordinates.
$\bar{V}_i$	Partial molar volume of species i.
x	Axial position along an idealized glomerular capillary, $0 \leq x \leq L$.
x_i	Mole fraction of species i.
z	Axial position along a pore, or coordinate perpendicular to the membrane surfaces, $0 \leq z \leq l$.

Greek Letters

α_{ij}	Phenomenological coefficients, Eq. 2.
$\beta(\zeta)$	Dimensionless concentration ratio, defined by Eq. 27.
$\gamma(\zeta)$	Modified pore Péclet number, defined by Eq. 52.
ζ	Dimensionless axial position along an idealized glomerular capillary, $0 \leq \zeta \leq 1$.
η	Viscosity of water, 0.007 g/(cm · s) at 37°C.
$\theta_S(\zeta), \theta_P(\zeta)$	Dimensionless solute and plasma protein concentrations, respectively, at any point along an idealized glomerular capillary.

θ_{SB}	Dimensionless solute concentration in Bowman's space.
$(\theta_{SB})_{\min}$	Minimum value of θ_{SB} achieved in the limit $Q_A \rightarrow \infty$.
$\bar{\theta}_S(\zeta)$	Dimensionless log mean solute concentration at any point along an idealized glomerular capillary, $(\theta_S - \theta_{SB})/\ln(\theta_S/\theta_{SB})$.
λ	Ratio of solute radius to pore radius, a/r_0.
Λ	Hydrodynamic force on a sphere, Eq. 43.
μ_i	Chemical potential of species i.
ξ_o	Ratio of pore-to-bulk solute diffusivity, Eq. 49.
π_A	Initial glomerular capillary (or afferent arteriolar) colloid osmotic pressure.
$\Delta\pi(x)$	The difference between colloid osmotic pressure at any point along an idealized glomerular capillary, and colloid osmotic pressure in Bowman's space.
ρ	Dimensionless radial coordinate within a pore, $0 \leq \rho \leq 1$.
σ	Reflection coefficient.
ϕ	Dissipation function per unit volume, the product of T and the volumetric rate of entropy production.
χ_o	Sieving coefficient, Eq. 50.
$\psi(\zeta)$	Dimensionless parameter, defined by Eq. 26.
ω	Solute permeability parameter, Eq. 6.

Subscripts

s, w, m	Solute, water, and membrane, respectively.

Mr. Chang is a predoctoral student in the Department of Chemical Engineering, Stanford University.
Dr. Deen is a Postdoctoral Research Fellow of the National Kidney Foundation.
Dr. Brenner is a Medical Investigator of the Veterans Administration.
This work was presented in part at the 66th Annual Meeting of the American Institute of Chemical Engineers, Philadelphia, Pa., 12 November 1973 (paper no. 57b), and at the 31st Annual Meeting of the American Federation for Clinical Research, Atlantic City, N. J., 4 May 1974 (*Clin. Res.* **22**:519A, 1974).

This study was supported in part by grants from the National Institutes of Health (HE14945 and AM 13888). Computer time was made available by the School of Engineering, Stanford University.

Received for publication 6 November 1974 and in revised form 14 March 1975.

REFERENCES

1. PAPPENHEIMER, J. R. 1953. Passage of molecules through capillary walls. *Physiol. Rev.* **33**:387.
2. RENKIN, E. M. 1954. Filtration, diffusion and molecular sieving through porous cellulose membranes. *J. Gen. Physiol.* **38**:225.
3. RENKIN, E. M., and J. P. GILMORE. 1973. Glomerular filtration. *Handbook Physiol.* **8**:185.
4. VERNIORY, A., R. DUBOIS, P. DECOODT, J. P. GASSÉE, and P. P. LAMBERT. 1973. Measurement of the permeability of biological membranes. Application to the glomerular wall. *J. Gen. Physiol.* **62**:489.
5. CHANG, R. L. S., I. F. UEKI, J. L. TROY, W. M. DEEN, C. R. ROBERTSON, and B. M. BRENNER. 1975. Permselectivity of the glomerular capillary wall to macromolecules. II. Experimental studies in rats using neutral dextran. *Biophys. J.* **15**:887.
6. DEEN, W. M., C. R. ROBERTSON, and B. M. BRENNER. 1972. A model of glomerular ultrafiltration in the rat. *Am. J. Physiol.* **223**:1178.
7. DEEN, W. M., C. R. ROBERTSON, and B. M. BRENNER. 1974. Concentration polarization in an ultrafiltering capillary. *Biophys. J.* **14**:412.
8. BRENNER, B. M., J. L. TROY, and T. M. DAUGHARTY. 1971. The dynamics of glomerular ultrafiltration in the rat. *J. Clin. Invest.* **50**:1776.
9. BRENNER, B. M., J. L. TROY, T. M. DAUGHARTY, W. M. DEEN, and C. R. ROBERTSON. 1972. Dynamics

of glomerular ultrafiltration in the rat. II. Plasma-flow dependence of GFR. *Am. J. Physiol.* **223:** 1184.

10. ROBERTSON, C. R., W. M. DEEN, J. L. TROY, and B. M. BRENNER. 1972. Dynamics of glomerular ultrafiltration in the rat. III. Hemodynamics and autoregulation. *Am. J. Physiol.* **223:**1191.
11. DEEN, W. M., J. L. TROY, C. R. ROBERTSON, and B. M. BRENNER. 1973. Dynamics of glomerular ultrafiltration in the rat. IV. Determination of the ultrafiltration coefficient. *J. Clin. Invest.* **52:**1500.
12. DAUGHARTY, T. M., I. F. UEKI, P. F. MERCER, and B. M. BRENNER. 1974. Dynamics of glomerular ultrafiltration in the rat. V. Response to ischemic injury. *J. Clin. Invest.* **53:**105.
13. MADDOX, D. A., W. M. DEEN, and B. M. BRENNER. 1974. Dynamics of glomerular ultrafiltration. VI. Studies in the primate. *Kidney Int.* **5:**271.
14. DEEN, W. M., D. A. MADDOX, C. R. ROBERTSON, and B. M. BRENNER. 1974. Dynamics of glomerular ultrafiltration in the rat. VII. Response to reduced renal mass. *Am. J. Physiol.* **227:**556.
15. MYERS, B. D., W. M. DEEN, C. R. ROBERTSON, and B. M. BRENNER. 1975. Dynamics of glomerular ultrafiltration in the rat. VIII. Effects of hematocrit. *Circ. Res.* **36:**425.
16. MADDOX, D. A., C. M. BENNET, W. M. DEEN, R. J. GLASSOCK, D. KNUTSON, T. M. DAUGHARTY, and B. M. BRENNER. 1975. Determinants of glomerular filtration in experimental glomerulonephritis in the rat. *J. Clin. Invest.* **55:**305.
17. LIGHTFOOT, E. N. 1974. Transport Phenomena and Living Systems. John Wiley & Sons, Inc., New York.
18. GAIZUTIS, M., A. J. PESCE, and J. E. LEWY. 1972. Determination of nanogram amounts of albumin by radioimmunoassay. *Microchem. J.* **17:**327.
19. PAPPENHEIMER, J. R., E. M. RENKIN, and L. M. BORRERO. 1951. Filtration, diffusion and molecular sieving through peripheral capillary membranes. A contribution to the pore theory of capillary permeability. *Am. J. Physiol.* **167:**13.
20. SOLOMON, A. K. 1968. Characterization of biological membranes by equivalent pores. *J. Gen. Physiol.* **51:**335s.
21. BEAN, C. P. 1972. The physics of porous membranes—neutral pores. *In* Membranes, Volume 1. Macroscopic Systems and Models. G. Eisenman, editor. Marcel Dekker, Inc., New York. 1–54.
22. ANDERSON, J. L., and J. A. QUINN. 1974. Restricted transport in small pores. A model for steric exclusion and hindered particle motion. *Biophys. J.* **14:**130.
23. KEDEM, O., and A. KATCHALSKY. 1958. Thermodynamic analysis of the permeability of biological membranes to nonelectrolytes. *Biochim. Biophys. Acta.* **27:**229.
24. SNELL, F. M., and B. STEIN. 1966. Onsager reciprocal relations in complex membranes. *J. Theor. Biol.* **10:**177.
25. ARTURSON, G., T. GROTH, and G. GROTTE. 1971. Human glomerular membrane porosity and filtration pressure: dextran clearance data analyzed by theoretical models. *Clin. Sci.* **40:**137.
26. GASSÉE, J. P. 1973. Effect of acetylcholine on glomerular sieving of macromolecules. *Pfluegers Arch. Gesamte Physiol.* **342:**239.
27. KATCHALSKY, A., and P. F. CURRAN. 1967. Nonequilibrium Thermodynamics in Biophysics. Harvard University Press, Cambridge, Mass.
28. KIRKMAN, H., and R. E. STOWELL. 1942. Renal filtration surface in the albino rat. *Anat. Rec.* **82:**373.
29. UZELAC, B. M., and E. L. CUSSLER. 1970. Diffusion of small particles through pores of similar diameter. *J. Colloid Interface Sci.* **32:**487.
30. SATTERFIELD, C. N., C. K. COLTON, and W. H. PITCHER, JR. 1973. Restricted diffusion in liquids within fine pores. *A.I.Ch.E. J.* **19:**628.
31. BECK, R. E., and J. S. SCHULTZ. 1972. Hindrance of solute diffusion within membranes as measured with microporous membranes of known pore geometry. *Biochim. Biophys. Acta.* **255:**273.
32. VAN BRUGGEN, J. T., J. D. BOYETT, A. L. VAN BEUREN, and W. R. GALEY. 1974. Solute flux coupling in a homopore membrane. *J. Gen. Physiol.* **63:**639.
33. BUNGAY, P. M., and H. BRENNER. 1973. Pressure drop due to the motion of a sphere near the wall bounding a Poiseuille flow. *J. Fluid Mech.* **60:**81.
34. HABERMAN, W. L., and R. M. SAYRE. 1958. Motion of rigid and fluid spheres in stationary and moving liquids inside cylindrical tubes. David Taylor Model Basin Report 1143. Dept. of the Navy, Washington, D.C.
35. WANG, H., and R. SKALAK. 1969. Viscous flow in a cylindrical tube containing a line of spherical particles. *J. Fluid Mech.* **38:**75.

APPENDIX[5]

Derivation of Flux Equations from Pore Theory

Eq. 1 can be transformed by noting that $N_i = \tilde{C}_i(v_i - v)$ (for definitions of these and other symbols see List of Symbols):

$$-\phi = \sum_{i=1}^{n} N_i(\mathrm{d}\mu_i/\mathrm{d}z) = \tilde{C}RT \sum_{i=1}^{n} (v_i - v)\,\mathrm{d}_i. \tag{33}$$

Eq. 33 defines a generalized mass transfer driving force, d_i:

$$\tilde{C}RTd_i = \tilde{C}_i(\mathrm{d}\mu_i/\mathrm{d}z) = \tilde{C}_i\{RT[\mathrm{d}(\ln a_i)/\mathrm{d}z] + \overline{V}_i(\mathrm{d}P/\mathrm{d}z)\}, \tag{34}$$

where the quantity $\tilde{C}RTd_i$ represents a force per unit volume of solution tending to move species i relative to the solution (17). As shown by Lightfoot (17), Eq. 33 together with the second and third postulates of nonequilibrium thermodynamics (linear relationships between fluxes and forces and reciprocity of the local phenomenological coefficients, respectively) may be used to obtain the Stefan-Maxwell equations:

$$d_i = \sum_{\substack{j=1 \\ j \neq k}}^{n} (x_i x_j / D_{ij})(v_j - v_k). \tag{35}$$

Combining Eqs. 34 and 35 and applying them to a ternary system composed of water, an uncharged solute, and a membrane, choosing $k = i$ and $v_m = 0$:

$$\begin{aligned} d_w &= F_{ws}x_w x_s(v_s - v_w) - f_{wm}x_w v_w, \\ &= x_w[(\mathrm{d}/\mathrm{d}z)(\ln a_w)]_{T,P} + (x_w\overline{V}_w/RT)(\mathrm{d}P/\mathrm{d}z), \end{aligned} \tag{36}$$

$$\begin{aligned} d_s &= F_{sw}x_s x_w(v_w - v_s) - f_{sm}x_s v_s, \\ &= x_s[(\mathrm{d}/\mathrm{d}z)(\ln a_s)]_{T,P} + (x_s\overline{V}_s/RT)(\mathrm{d}P/\mathrm{d}z), \end{aligned} \tag{37}$$

where

$$\begin{aligned} F_{sw} &= F_{ws} = D_{sw}^{-1} = D_{ws}^{-1}, \\ f_{sm} &= x_m/D_{sm}, \quad f_{wm} = x_m/D_{wm}. \end{aligned} \tag{38}$$

As shown by Eqs. 36–38, three frictional coefficients (F_{sw}, f_{sm}, and f_{wm}) are required in general to describe mass transport in this system. Adding Eqs. 36 and 37 in such a way as to eliminate the $\mathrm{d}P/\mathrm{d}z$ terms, it can be shown that the molar flux of solute relative to the membrane

[5] The authors are indebted to Dr. E. N. Lightfoot for pointing out that the Stefan-Maxwell equations could serve as a basis for the derivation of flux relations using pore theory. This suggestion provided the principal motivation for the development presented here.

$(\tilde{C}_s v_s)$ is given by

$$\tilde{C}_s v_s = -K^{-1}\mathfrak{D}_s (d\tilde{C}_s/dz) + \tilde{C}_s v_w G. \tag{39}$$

Assuming that the solution is ideal and dilute,

$$K^{-1}\mathfrak{D}_s = 1/(F_{sw} + f_{sm}), \tag{40}$$

$$G = [F_{sw} + (\bar{V}_s/\bar{V}_w) f_{wm}]/(F_{sw} + f_{sm}). \tag{41}$$

An expression for the water velocity is obtained by simply adding Eqs. 36 and 37 and using the Gibbs-Duhem relation to eliminate terms involving the activities (a_s and a_w):

$$v_w = -(1/\tilde{C}RTf_{wm})(dP/dz) \tag{42}$$

where again the solution is assumed to be dilute.

Explicit relationships for the frictional coefficients may be obtained by assuming that transport takes place through cylindrical pores (Fig. 1) and applying results from low Reynolds number hydrodynamics. Bungay and Brenner (33) recently demonstrated that for a solid sphere of arbitrary size and position within a long cylindrical tube at low Reynolds number, the hydrodynamic force on the sphere (Λ) and the additional pressure drop force due to the presence of the sphere ($\Delta P^+ A$) are both linear functions of the translational velocity of the sphere (v_s) and the mean fluid velocity. Since it is assumed in the present study that the volume fraction of solute is very small, the mean fluid velocity is essentially identical to the volumetric average velocity (J_v'). Thus, for a freely suspended and neutrally buoyant particle (zero torque):

$$\begin{pmatrix} \Lambda \\ \Delta P^+ A \end{pmatrix} = -\eta \begin{pmatrix} R_{11} & R_{12} \\ R_{21} & R_{22} \end{pmatrix} \begin{pmatrix} v_s \\ -J_v' \end{pmatrix}. \tag{43}$$

The R_{ij} are hydrodynamic resistance coefficients which are functions only of the sphere and tube radii and the position of the sphere, and which have the property $R_{12} = R_{21}$. Accordingly, the pressure gradient in a tube containing solid spheres may be written as

$$dP/dz = (dP^\circ/dz) + (\Delta P^+/l) \tag{44}$$

where

$$dP^\circ/dz = -8\eta J_v'/r_o^2 \tag{45}$$

is the pressure gradient in unperturbed Poiseuille flow.

The resistance coefficients R_{ij} have been computed by Haberman and Sayre (34) for the special case of a sphere moving along the tube axis (sphere at $\rho = 0$) for $\lambda < \sim 0.8$. Under these conditions, Wang and Skalak (35) have shown that the excess pressure gradient due to the sphere, $\Delta P^+/l$, is less than 2% of the Poiseuille pressure gradient provided that $\lambda < 0.8$. In addition, Bungay and Brenner (33) considered the additional pressure drop created by a relatively small sphere moving near the wall of a circular tube through which there is a Poiseuille flow. For the

limited number of cases reported ($\lambda < 0.1$ and sphere position such that $\lambda/(1 - \rho) < \sim 0.25$), the excess pressure drop due to the sphere is again small compared with the Poiseuille pressure drop, provided that l/r_o is large (33). Taken together, these hydrodynamic results (33, 35) suggest that the term $\Delta P^+ A$ in Eq. 43 is negligible for a variety of sphere sizes and positions. Furthermore, given that $A = (\tilde{N}\tilde{C}_s l)^{-1}$, it can be shown from Eq. 43 that

$$\Delta P^+/l = -\tilde{N}\tilde{C}x_s\eta(R_{21}v_s - R_{22}J_v'). \tag{46}$$

Consequently, provided that $\lambda < 1$ to assure that R_{21} and R_{22} remain finite, $\Delta P^+/l$ will be negligible if the solution is sufficiently dilute ($x_s \ll 1$). Under these conditions ($\Delta P^+/l \simeq 0$), the pressure gradient in Eq. 42 is the same as that in unperturbed Poiseuille flow, so that

$$f_{wm} = (4\eta/\tilde{C}RTr_o^2)[1/(1 - \rho^2)]. \tag{47}$$

Integrating Eq. 39 over the pore cross section, noting from Eqs. 42, 45, and 47 that $v_w = 2J_v'(1 - \rho^2)$, gives the solute flux equation used by Anderson and Quinn (22):

$$J_s' = -\xi_o \mathfrak{D}_\infty (d\hat{C}_s/dz) + \chi_o \hat{C}_s J_v', \tag{48}$$

where J_s' is the average solute mass flux, based on the pore area. In applying Eq. 48, the hindrance terms for diffusion (ξ_o) and convection (χ_o) are evaluated from results obtained for spheres located along the axis of a tube (22):

$$\xi_o = (1 - \lambda)^2 K^{-1}(\lambda, 0), \tag{49}$$

$$\chi_o = (1 - \lambda)^2[2 - (1 - \lambda)^2]G(\lambda, 0). \tag{50}$$

ξ_o, the ratio of the solute diffusivity in the pore to that in free solution, and χ_o, the sieving coefficient expressing the hindrance of the pore to convective solute transport, are both generally less than one. When the radius of the pore greatly exceeds that of the solute molecule, Eq. 48 reduces to the solute flux equation applicable to unbounded solutions (i.e., ξ_o and $\chi_o \to 1$ as $\lambda \to 0$), as expected. In this case, f_{wm} and $f_{sm} \to 0$ and $F_{sw} \to \mathfrak{D}_\infty^{-1}$. The functions $K^{-1}(\lambda, 0)$ and $G(\lambda, 0)$, which represent frictional hindrances, have been tabulated for $\lambda \leq 0.80$ (35). The terms which multiply K^{-1} and G in Eqs. 49 and 50 account for steric exclusion of the solute particle.

Integration of Eq. 48 along the pore provides an expression for the solute concentration profile in the pore, $\hat{C}_s(z)$. Substituting this into Eq. 48 and averaging along the pore, while keeping separate the terms representing diffusion and convection, leads to the following:

$$J_s = \underbrace{\frac{S'}{S}\frac{\xi_o \mathfrak{D}_\infty}{l}(C_o - C_l)}_{\text{diffusion}} + \underbrace{\chi_o J_v C_o\left[\frac{1 - (C_l/C_o)\exp(-\gamma)}{1 - \exp(-\gamma)}\right] - \frac{S'}{S}\frac{\xi_o \mathfrak{D}_\infty}{l}(C_o - C_l)}_{\text{convection}}, \tag{51}$$

where

$$\gamma = \chi_o J_v' l / \xi_o \mathfrak{D}_\infty . \tag{52}$$

Eq. 51 for J_s (now based on total surface area) reduces to Eq. 4 since the terms involving $\mathfrak{D}_\infty$ cancel. For the case when $J_v = 0$, Eqs. 4 and 51 have the limiting form:

$$J_s = (S'/S)(\xi_o \mathfrak{D}_\infty / l)(C_o - C_l). \tag{53}$$

The expression for the volume flux, J_v (Eq. 3), is obtained by integrating Eq. 42 over the pore cross section and length (evaluating f_{wm} from Eq. 47), and noting that the net driving pressure is given by the difference between transmembrane hydraulic and colloid osmotic pressures ($\Delta P - \Delta\pi$) rather than by ΔP alone.

In summary, use of the Stefan-Maxwell equations makes it clear that three frictional coefficients are needed to describe mass transport in a system composed of water, an uncharged macromolecular solute, and a membrane. If the local coefficients (F_{sw}, f_{wm}, and f_{sm}) are averaged over the entire membrane, overall coefficients are obtained which are analogous to those derived from the Kedem-Katchalsky formulation (K_f, ωS, and σ). Representation of the transport pathways as identical cylindrical pores and the solute molecules as solid spheres (Fig. 1) allows these overall coefficients to be expressed in terms of a different set of three physical parameters (r_o, S'/l, and η). The principal advantage of this transformation, brought about using isoporous theory, is that η may be determined independently of the membrane, leaving only r_o and S'/l to be evaluated from membrane transport experiments. As discussed in the companion study (5), this has the practical effect of allowing the membrane parameters based on pore theory (K_f, r_o, and S'/l) to be evaluated in a single experiment, whereas data from at least two experimental conditions (e.g., normal hydropenia and plasma volume expansion) are needed to evaluate the Kedem-Katchalsky parameters (K_f, ωS, and σ).